

## Direct Virtual Power Control

Li Xiang\*, Han Minxiao

State Key Laboratory of Alternate Electrical Power System with Renewable Energy Sources

School of Electrical & Electronic Engineering

North China Electric Power University

Beijing China

\*Corresponding author, e-mail: xiang.lee.c@gmail.com

### Abstract

A direct virtual power control algorithm is presented in this paper for VSC-HVDC startup. This control algorithm is based on direct power control (DPC) and expands the range of DPC. When the VSC converter AC side open circuit or the AC side current is zero, the control algorithm maintains the DPC feedback loop by introducing a virtual power, so that the DPC is able to control the AC output voltage amplitude and frequency stability before the VSC converter connecting to the grid network and keep consistent with the grid connection point. This algorithm process is simple, containing most of the DPC control module, and consistent with the DPC structure. Therefore, the control algorithm switches smoothly before and after the VSC converter connecting to the grid. This paper uses PSCAD / EMTDC software platform and laboratory hardware circuit experiments to test and verify the correctness and validity of the control algorithm.

**Keywords:** VSC-HVDC, starting-up, grid integration, virtual power

**Copyright © 2014 Institute of Advanced Engineering and Science. All rights reserved.**

### 1. Introduction

In recent years, voltage source converter high voltage direct current (Voltage Source Converter High Voltage Direct Current, VSC-HVDC) technology is developing rapidly, it is tremendous prospect of transmission and distribution solutions for the modern power system [1]. It is a new transmission system that is suitable for grid interconnection, isolated power supply, large-scale renewable energy grid-connection and etc [2-6]. With the rapid development of renewable energy and distributed power, VSC-HVDC technology will have to be a further development and application.

Researches on VSC-HVDC control algorithm have been developing recent years, which is based on the theory of current control. Through the rotating axis oriented by the voltage or the virtual flux, current control makes the AC side current decoupled into active and reactive current component, with relatively low static error and better dynamic response [7]. But this control algorithm operation is dependent on the system parameters accuracy, and problems are more complicated on the current loop control strategy [8]. Based on the principle of direct torque control, a new control algorithm is developed, which is direct power control (Direct Power Control, DPC). This control algorithm doesn't need PI controller and current inner loop control. It can compute the control output according to the virtual flux and instantaneous reactive and active power, so it has the advantages of simple control structure, fast dynamic response, etc [9, 10]. But before the VSC-HVDC converter starting grid-connection, the converter AC side is equivalent to open circuit with no current. If the DPC take control, the control module will lose control feedback input, so that the entire control algorithm does not work. This article is based on the algorithm of direct power control with space vector modulation (Direct Power Control with Space Vector Modulation, DPC-SVM), proposes a direct virtual power control algorithm that is applied to the VSC converters startup and grid-connection control. When the AC side current is zero, the network control is using the virtual converter output power approaches to keep the feedback path of DPC module, thereby DPC algorithm is able to effectively control the AC side voltage stable before VSC converter starting grid-connection. The characteristics of this control algorithm are the structure is simple, using most common calculation and control unit together with the original SVM-DPC, basic structure of the network controller remains the same before

and after the converter startup and grid-connection and the control algorithm is switching smoothly.

**2. VSC-HVDC System Startup Process Description**

Its startup process is firstly connecting one side inverter to the grid through a current limiting resistor, blocking the IGBT starting pulse, recharging to the DC side by using six anti-diode structured rectifier circuit. When the DC charge reaches a predetermined voltage, releasing pulse blockade, and begin to control the DC voltage stabilized by control algorithms. The other side of the converters is necessary to control the AC side voltage amplitude, frequency keeping constant with the grid voltage amplitude and frequency, then connect to the grid [1, 11].

The control algorithm presented in this paper is to control the other side of the converter voltage stability after the DC voltage stabled, and keep the voltage the same with the grid. This control algorithm uses the structure of DPC-SVM algorithm to reduce and control the fluctuations caused by the control algorithm switching process during the network connection.

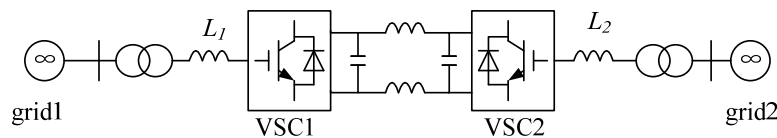


Figure 1. Proposed Circuit of the VSC-HVDC System

$L_1$  and  $L_2$  in figure 1 are reactances between the converters and grids.

**3. DPC-SVM Based on the Virtual Flux**

There are already some articles on DPC control algorithm, which [12-18] is about the traditional DPC control algorithm based on switch tables, and [19-21] is about improved DPC-SVM, but in this paper, the presented control algorithm is based on the second algorithm, because the frequency of DPC-SVM control switch is fixed and has better transient characteristics. According to the introduction of the article [19-21], the calculation process of virtual flux obtains DPC-SVM.

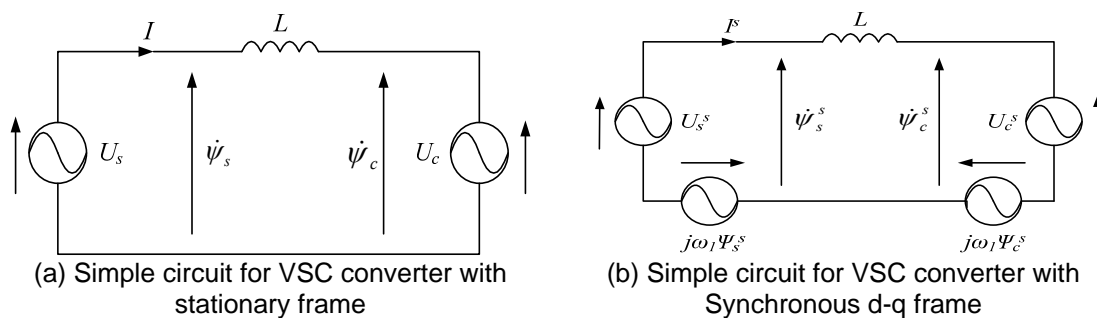


Figure 2. Equivalent Circuit of a Grid Connected VSC Converter

In Figure 2(a),  $\Psi_s$  and  $\Psi_c$  are the vectors of grid flux and converter flux;  $U_s$  and  $U_c$  are the vectors of grid voltage and converter output AC voltage;  $I$  is the vector of the converter AC side current; in Figure 2(b), the vectors by adding the superscript  $s$  is the corresponding quantities on the synchronous axes;  $\omega_1$  is synchronous frequency;  $L$  is reactance between the converter and grid.

Imagine the VSC converter to be an ideal voltage source and connecting to the grid, the simplified equivalent circuit is shown in Figure 2(a) above. The same as motor flux definition, the grid flux  $\Psi_s$  and the converter flux  $\Psi_c$  can be defined as:

$$\begin{cases} \Psi_s = \int U_s dt \\ \Psi_c = \int U_c dt \end{cases} \quad (1)$$

According to Figure 2(a) and Equation (1), it shows that:

$$\Psi_s = L * I + \Psi_c \quad (2)$$

The system shown in Figure 2(a) can be converted to synchronous coordinate with the synchronous rotating speed  $\omega_1$ , as shown in Figure 2(b). The following equation can be obtained from Figure 2(b) and Equation (2):

$$\Psi_s^s = L * I^s + \Psi_c^s \quad (3)$$

$$\begin{cases} U_s^s = \Psi_s^s + j\omega_1 \Psi_s^s \\ U_c^s = \Psi_c^s + j\omega_1 \Psi_c^s \end{cases} \quad (4)$$

From Equation (3), the inflow grid current can be calculated through the flux:

$$I^s = \frac{\Psi_s^s - \Psi_c^s}{L} \quad (5)$$

From the grid direction, the converter output active and reactive power  $P_s$  and  $Q_s$  is:

$$P_s - jQ_s = \frac{3}{2} U_s^s * I^s \quad (6)$$

The d-q axes of the rotating coordinate uses the direction of the grid flux  $\Psi_s$  as a reference, as shown in Figure 2(b):

$$\Psi_{sd} = |\Psi_s|, \quad \Psi_{sq} = 0 \quad (7)$$

The grid voltage and frequency is constant, so:

$$\frac{d\Psi_s^s}{dt} = \frac{d\Psi_{sd}}{dt} = 0 \quad (8)$$

Take the formula (4), (5) and (7) into (6) to get the active and reactive power:

$$P_s - jQ_s = \frac{3}{2L} \omega_1 \Psi_{sd} [-\Psi_{cq} - j(\Psi_{cd} - \Psi_{sd})] \quad (9)$$

Thus the formula can be obtained as below:

$$\begin{cases} P_s = -\frac{3}{2L} \omega_1 \Psi_{sd} \Psi_{cq} \\ Q_s = \frac{3}{2L} \omega_1 \Psi_{sd} (\Psi_{cd} - \Psi_{sd}) \end{cases} \quad (10)$$

$\Psi_{sd}$  and  $\omega_1$  are constants, because the grid voltage is constant, the Equation (10) can be differentiated to get:

$$\begin{cases} \frac{dP_s}{dt} = -\frac{3}{2L} \omega_1 \Psi_{sd} \frac{d\Psi_{cq}}{dt} \\ \frac{dQ_s}{dt} = \frac{3}{2L} \omega_1 \Psi_{sd} \frac{d\Psi_{cd}}{dt} \end{cases} \quad (11)$$

From the formula (1), the relationship between the flux and the voltage vector is:

$$\frac{d\Psi_c}{dt} = U_c \quad (12)$$

It can be seen from the formula (11) and (12), adjusting output voltage vector of the converter during the sampling period  $T_s$ , it is able to reduce the power error to zero.

When the sampling period  $T_s$  is small enough, discrete the Equation (11), so that in  $T_s$ , the changes of the active and reactive power are:

$$\begin{cases} \Delta P_s = -\frac{3}{2L} \omega_1 \Psi_{sd} \Delta \Psi_{cq} \\ \Delta Q_s = \frac{3}{2L} \omega_1 \Psi_{sd} \Delta \Psi_{cd} \end{cases} \quad (13)$$

From Equation (13), it can be seen the changes of active and reactive power in  $T_s$  are determined respectively by the changes of the converter flux within the same period and which is shown through the  $\Delta \Psi_{cq}$  of the q-axis component and  $\Delta \Psi_{cd}$  of the d-axis component on the synchronized axes.

In the steady-state process, the power error in  $T_s$  can be gotten through the reference values of the active power  $P_s^*$  and reactive power  $Q_s^*$ :

$$\begin{cases} \Delta P_s = P_s^* - P_s \\ \Delta Q_s = Q_s^* - Q_s \end{cases} \quad (14)$$

The formula (13) shows that reduce the power error to 0, it can also be using the method of changing the converter flux on the d-q axis component. By the formula (13) the size of the desired changes of the flux can be calculated:

$$\begin{cases} \Delta \Psi_{cq} = -\frac{2L}{3\omega_1 \Psi_{sd}} \Delta P_s \\ \Delta \Psi_{cd} = \frac{2L}{3\omega_1 \Psi_{sd}} \Delta Q_s \end{cases} \quad (15)$$

By the formula (4) it can be obtained:

$$\frac{d\Psi_c^s}{dt} = U_c^s - j\omega_1 \Psi_c^s \quad (16)$$

According to formula (16), as the sampling time is short enough, the differential value of the converter flux equals to the value of the changes approximately within the sampling period:

$$\Delta \Psi_c^s = U_c^s * T_s - j\omega_1 \Psi_c^s * T_s \quad (17)$$

By the formula (17) it can be obtained:

$$\begin{cases} \Delta \Psi_{cq} = U_{cd} * T_s + \omega_1 \Psi_{cq} * T_s \\ \Delta \Psi_{cd} = U_{cq} * T_s - \omega_1 \Psi_{cd} * T_s \end{cases} \quad (18)$$

From the formula (18), the value of the output target voltage of the converter can be obtained during the sampling time period  $T_s$  is:

$$\begin{cases} U_{cd}^* = -\omega_l \Psi_{cq} + \frac{\Delta \Psi_{cq}}{T_s} \\ U_{cq}^* = \omega_l \Psi_{cd} + \frac{\Delta \Psi_{cd}}{T_s} \end{cases} \quad (19)$$

Combine the formula (13) and (19), the converter target voltage value on the rotating synchronous axis in a sampling period  $T_s$  can be gotten from the power change:

$$\begin{cases} U_{cd}^* = -\omega_l \Psi_{cq} + \frac{2L\Delta Q_s}{3T_s \omega_l \Psi_s} \\ U_{cq}^* = \omega_l \Psi_{cd} - \frac{2L\Delta P_s}{3T_s \omega_l \Psi_s} \end{cases} \quad (20)$$

As can be seen from the calculation equation of the target voltage, the value of the target voltage is calculated from the power error, so that both of the active and reactive power is mastered. Compare to voltage vector control algorithm, the current does not need to be controlled, the calculation process only involves simple multiplication and division without complex mathematics calculation. The block diagram about the DPC-SVM control algorithm is shown in Figure 3.

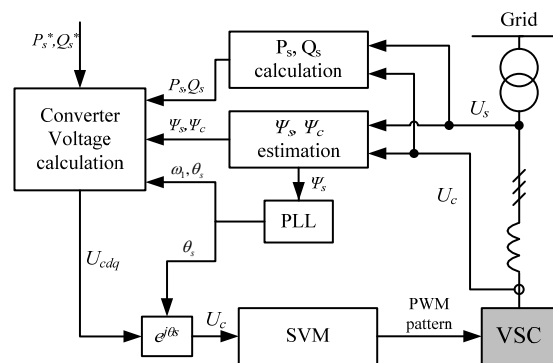


Figure 3. Schematic Diagram of DPC-SVM

#### 4. Direct Virtual Power Control

The above is an introduction to DPC-SVM control algorithm. As the first part of the analysis shown that before the VSC converter connecting to the grid, the AC side of the converter is an open circuit, the converter input and output active and reactive power is constantly to be zero. Thus DPC-SVM control loses the effective feedback path, therefore, DPC-SVM algorithm does not work normally in this case. As a result it is not be able to remain the converter AC side output voltage stability and achieve a soft grid-connection. To enable DPC work before the VSC converter connecting to the grid, the virtual power is introduced in this paper which makes sure the DPC-SVM having an effective feedback loop in case of the converter AC side at an open circuit state, and achieves the control to the AC side output voltage.

The information of the grid voltage amplitude and frequency should be contained by the virtual power. Firstly, take the grid voltage as a reference input  $U_s$ , then virtualizes a current with the same direction as the converter, the amplitude of this virtual current is  $I_v = -\frac{T_s \omega_l \Psi_s}{L}$ .  $\Psi_s$  in the virtual current can be calculated by the grid voltage vector, so this virtual current includes the amplitude information of the grid voltage. Several other parameters are constants, which can be eliminated during the target voltage calculation process of the original DPC-SVM algorithm

control. Finally the target voltage which includes the information of the converter output voltage and the grid voltage is obtained through the virtual power calculation.

Since this current does not exist, it will not affect the size of and the relative relations between other electric parameters but only introducing a virtual power, in order to achieve the purpose of establishing DPC-SVM control algorithm for power feedback path. Choose the direction of the rotating synchronous axis the same as the grid flux direction, due to the flux of the converter AC side open circuit at steady state is consistent with the grid flux direction, and the converter voltage vector direction is behind the converter flux vector 90 degrees, virtual power can be obtained by the virtual current. Since the direction of the current and the voltage is the same, the virtual reactive power  $Q_{sv}$  should be 0, and the virtual active power  $P_{sv}$  should be:

$$\begin{cases} P_{sv} = \frac{3}{2}U_{sv} * I_v = \frac{3}{2}U_c * I_v \\ = -\frac{3T_s\omega_l\Psi_s U_c}{2L} \\ Q_{sv} = 0 \end{cases} \quad (21)$$

Set the reference value of the virtual power as:

$$\begin{cases} P_{sv}^* = -\frac{3T_s\omega_l\Psi_s U_s}{2L} \\ Q_{sv}^* = 0 \end{cases} \quad (22)$$

Calculating the virtual power error by using the value of reference virtual power and virtual power:

$$\begin{cases} \Delta P_{sv} = -\frac{3T_s\omega_l\Psi_s (U_c - U_s)}{2L} \\ \Delta Q_{sv} = 0 \end{cases} \quad (23)$$

Take the error values of the virtual power into the formula (20), and by using the original DPC-SVM target voltage calculation module to get the result:

$$\begin{cases} U_{cd}^* = -\omega_l\Psi_{cq} \\ U_{cq}^* = \omega_l\Psi_{cd} - \frac{2L\Delta P_{sv}}{3T_s\omega_l\Psi_s} \end{cases} \quad (24)$$

As the converter flux and the grid flux is in the same direction, so:

$$\Psi_{cq} = 0, \quad \Psi_{cd} = |\Psi_c| \quad (25)$$

Take the formula (23) and (25) into equation (24), the target voltage value can be obtained:

$$\begin{cases} U_{cd}^* = 0 \\ U_{cq}^* = \omega_l\Psi_c - \frac{2L\Delta P_{sv}}{3T_s\omega_l\Psi_s} \\ = \omega_l\Psi_c - \frac{2L}{3T_s\omega_l\Psi_s} * \frac{3T_s\omega_l\Psi_s (U_c - U_s)}{2L} \\ = \omega_l\Psi_c - (U_c - U_s) \\ = \omega_l\Psi_c + \Delta U_c \end{cases} \quad (26)$$

The final formula (26) about the target voltage calculation shows that because of the introduction of a virtual power, the converter power feedback path can be established in the situation when the converter AC side current flow is zero, and allows DPC algorithm play a role. The results obtained through the calculation process shows that the entire control process is very simple, and just need a little modification to DPC-SVM algorithm which is only adding a virtual power calculation module, so that the process can be controlled to switch smoothly before and after the VSC converter startup and connecting to the grid. In order not to change power error calculation of the real power control module and the reference input, a compensation is added to the reference virtual power, and the compensation is  $\frac{3T_s \omega_l \Psi_s U_s}{2L}$ . The entire control algorithm block diagram is shown in Figure 4:

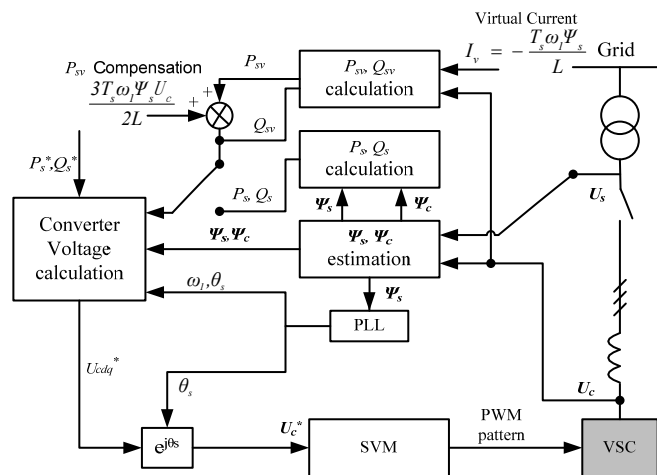


Figure 4. Schematic Diagram of the Proposed Direct Virtual Power Control

**5. Experimental Verification**

In order to verify the effectiveness of the proposed VSC-HVDC control algorithm, the authors do the studies and analysis from two angles of the digital simulation and physical experiments. Firstly, doing the simulation experiments on PSCAD/EMTDC software platform. The simulation set on both sides of VSC converter rated transmission power at 200MW, the AC side rated voltage at 230kV, DC bus voltage at 400kV, and the reactor on both sides of the network at 0.07H. Control algorithm verification test carries out after one side of the VSC converters startup and the DC voltage is stable, grid-connecting starts at the simulation time of 0.5s. In order to reduce the current impact, control the transmission power after grid-connection to 0MW. Then increase the transmission power to 200MW at 0.8s. Through this process, observe the stability of the converter AC side output voltage, current and the processes of grid-connection and the control algorithms switching.

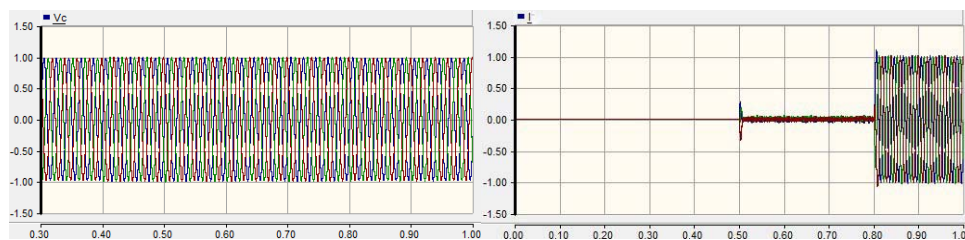


Figure 5. AC Voltage and AC Current of the VSC Converter

As can be seen from Figure 5, before the converter connecting to the grid, the amplitude and frequency are stable when using the direct virtual power control algorithm to control the converter AC side output voltage. There is only very small fluctuations on the converter AC side output voltage and current before and after the grid-connection. This results indicate that the proposed control algorithm is effective and achieves a smooth switch before and after the grid-connection.

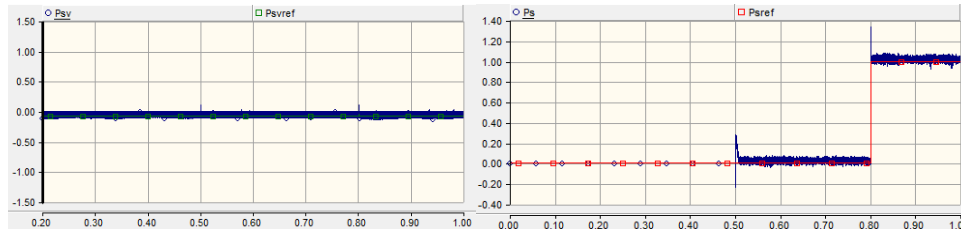


Figure 6. Virtual Power and Output Power of the Converter AC Side

It can be seen from the virtual power curve, before the grid-connection, the direct virtual power control algorithm controls the converter AC side voltage remain stable by tracking the output virtual power. And the converter AC side output curve shows there are small fluctuations on output power during the grid-connection. After the grid-connection, the control method switches direct virtual power control to DPC with a smooth handover process. Thus, DPC is able to effectively control the output power of the converter.

Based on the simulation experiments, build a physics experimental circuit under the laboratory environment to verify the effectiveness of the algorithm.

The test circuit structure does a certain simplification to the simulation system circuit structure, which the DC side using lithium battery powering, and the converter is connected to the 380V grid through the 0.5mH grid reactors and transformer with variable ratio of 260V/400V, the system rated capacity is 50kVA. The experimental circuit device is shown in Figure 7.

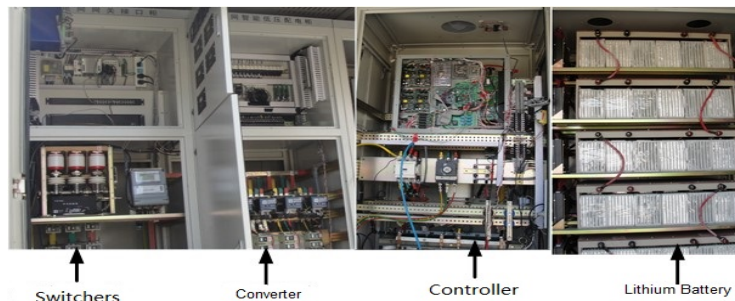


Figure 7. The Photos of Experimental Setups

To do the network test and power adjustment test based on this experimental system. Firstly, use the oscilloscope to get the traces of the both sides voltage of the breaker and the current of the converter AC side.

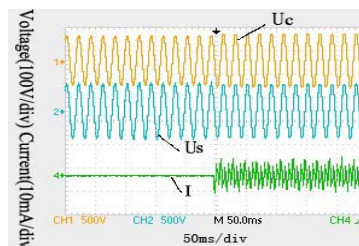


Figure 8. AC Voltage and AC Current at the Cutting-in Moment

The traces show, before the grid-connection, the control algorithm finely controls the converter output voltage in consistent with the amplitude, frequency and phase of the grid AC voltage, so that the grid-connection process is smoothly completed. Meanwhile the converter control algorithms switch smoothly from the direct virtual power control before the grid-connection state to DPC.

Then do the experiment on network output power adjustment. Adjust the converter output power from 2kW to 9kW. Record the voltage and current traces of the transient process in Figure 9.

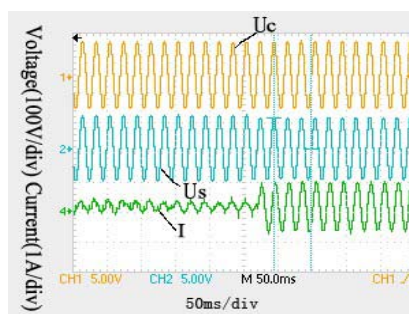


Figure 9. AC Voltage and AC Current at the Moment of Changing the Output Power

From the traces it can be seen that DPC can effectively control the size of the converter AC side power output.

## 6. Conclusion

This article is about DPC problem of lack of control on the AC voltage stability before the VSC-HVDC converter startup, and the authors propose the approach of establishing a feedback loop made by the virtual power. This method does minimal changes to the structure of DPC-SVM control algorithm and introduces the virtual power as the input. It makes the traditional DPC-SVM algorithm to be able to control the AC side output voltage remaining stable before the converter connecting to the grid. Also its calculation process and algorithm structure is relatively simple and having a fast dynamic response. It proves that the simulation and physical circuit tests having the validity on this algorithm, and can be smoothly switched before and after the converter connecting to the grid.

## Acknowledgements

This work was supported by National Key Technology R&D Program of the Ministry of Science and Technology of China (Grant No. 2009BAA22B01).

## References

- [1] Zhang Jing, Xu Zheng, Chen Hairong. Startup Procedures for the VSC-HVDC System. *Transactions of China Electrotechnical Society*. 2009; 09:159-165.
- [2] Xiang Li, Minxiao Han. A coordinated control strategy of series multi-terminal VSC-HVDC for offshore wind farm. *Transactions of China Electrotechnical Society*. 2013; 05: 42-48+57.
- [3] Haileselassie TM, Torres-Olguin RE, Vrana TK, Uhlen K, Undeland T. Main grid frequency support strategy for VSC-HVDC connected wind farms with variable speed wind turbines. *Power Tech., IEEE Trondheim*. 2011.
- [4] Yao Xing-jia, Ding Yang, Guo Qing-ding. Research on application of VSC-HVDC system in the offshore wind farm. *Renewable Energy Resources*. 2012; 02: 37-41.
- [5] Olawole Joseph Petinrin, Mohamed Shaaban. Overcoming Challenges of Renewable Energy on Future Smart Grid. *TELKOMNIKA Indonesian Journal of Electrical Engineering*. 2012; 10(2): 229-234

- [6] Yogendra Arya, Narendra Kumar, Hitesh Dutt Mathur. Automatic Generation Control in Multi Area Interconnected Power System by using HVDC Links. *International Journal of Power Electronics and Drive Systems*. 2012; 2(1): 67-75
- [7] Li Shuang, Wang Zhixin, Wang Guoqiang. Predictive Direct Power Control Strategy for Offshore Wind Power VSC-HVDC Converter. *Transactions of China Electrotechnical Society*. 2013; 02: 264-270.
- [8] Xiao L, Huang S, Lu K. DC-bus voltage control of grid-connected voltage source converter by using space vector modulated direct power control under unbalanced network conditions. *Power Electronics IET*. May 2013; 6:5.
- [9] Alonso-Martinez J, Eloy-Garcia J, Santos-Martin D, Arnaltes S. A New Variable-Frequency Optimal Direct Power Control Algorithm. *IEEE Transactions on Industrial Electronics*. April 2013; 60(4): 1442, 1451.
- [10] Yongchang Zhang, Zhengxi Li, Yingchao Zhang, Wei Xie, Zhengguo Piao, Changbin Hu. Performance Improvement of Direct Power Control of PWM Rectifier With Simple Calculation. *IEEE Transactions on Power Electronics*. 2013; 28(7): 3428, 3437.
- [11] Chen Hai-rong, Zhang Jing, Pan Wu-lue. Start-up Control of VSC Based on HVDC System. *High Voltage Engineering*. 2009; 05: 1164-1169.
- [12] WANG Jiu-he, LI Hua-de, WANG Li-ming. Research on direct power control for three phase boost-type pwm rectifier. Proceedings of the CSEE, 2006; 18:54-60.
- [13] Xie Lei, Xie Da, Zhang Yanchi, Ai Qian, Wang Zhixin. VSC-HVDC System Based on VF-DPC. *Electric Power Science and Engineering*. 2009; 01: 14-18.
- [14] ZHAO Huan, WANG Hong-mei. Novel Modulation Strategy of Direct Power Control of PWM Rectifier Based on Virtual Flux. *Industry and Mine Automation*. 2009; 01: 14-18.
- [15] ZHAI Li-li, BU Wen-shao, WANG Shao-jie. Fixed Frequency VF-DPC of Three-phase Voltage-type PWM Rectifier. *Electrical Measurement & Instrumentation*. 2012; 05:25-28.
- [16] LU Jian-kang, XING Yi-xun. Improved Direct Power Control Strategy for Three - phase PWM Rectifier. *Computer Simulation*. 2012; 08: 291-295.
- [17] HU Xue-gang, DAI Xun-jiang. Direct Power Control of Grid-Connected Inverters Based on Virtual Flux. *Power System and Clean Energy*. 2012; 10: 87-91.
- [18] WANG Yun-liang, ZHAO Yong-le. Research of improved virtual-flux-based direct power control. *Chinese Journal of Power Sources*. 2013; 04: 668-671.
- [19] Lie Xu, Dawei Zhi, Liangzhong Yao. *Direct Power Control of Grid Connected Voltage Source Converters*. Power Engineering Society General Meeting. 2007.
- [20] SHI Jian-xin, JIAO Zhen-hong, DONG Jin-bao, LI Lin-jie. Research on PWM Rectifier with Direct Power Control based on Space-Vector Modulation. *Small & Special Electrical Machines*. 2010; 07: 60-62.
- [21] SONG Shu-zhong, SHAN Dong-liang, MA Jian-wei, WANG Xian-bo. Direct power control with constant switching frequency for PWM rectifier. *Chinese Journal of Power Sources*. 2011; 02: 215-217.